


Access provided by:
**INSTITUTE OF COMPUTING
TECHNOLOGY CAS**
Sign Out

Browse

My Settings

Get Help

QUICK
PREVIEW

Abstract

Authors

Figures

Multimedia

References

Cited By

Keywords

Portable coherent frequency-modulated continuous-wave radar for indoor human tracking

Radar-based human tracking can be applied to indoor healthcare scenarios, such as fall detection of elderly people. In this work, a portable frequency-modulated continuous-wave (FMCW) radar prototype for indoor human tracking is presented. The system provides absolute-range detection capabilities. Furthermore, it uses a novel approach - not requiring the sharing of the generation and acquisition clocks - to possess the highly-desired coherence feature, which enables the preservation of the phase history of targets. As a result, videos of inverse synthetic aperture radar (ISAR) images - i.e., videos of range-Doppler frames - can be reconstructed. Experimental results for a walking person in a highly-cluttered indoor environment confirm the suitability of the low-cost radar prototype for indoor healthcare applications.

This paper appears in: 2016 IEEE Topical Conference on Biomedical Wireless Technologies, Networks, and Sensing Systems (BioWireless), Issue Date: 24-27 Jan. 2016, Written by: Zhengyu Peng; Jos?-Mar?a Mu?oz-Ferreras; Yao Tang; Roberto G?mez-Garc?a; Changzhi Li

© 2016 IEEE

SECTION I INTRODUCTION

The application of radars to indoor scenarios is becoming highly appealing [1]. In particular, Doppler radars have emerged as adequate devices to detect the presence of humans or even to monitor vital signs [2]. An interesting application to improve the quality of life of elderly people is the detection of unfortunate falls [3], [4].

Doppler radars do not possess range resolution—i.e., they do not transmit instantaneous bandwidth—and hence, they cannot obtain absolute ranges of targets. Conversely, they can obtain precise Doppler information related to the target radial velocity [2]. Frequency-modulated continuous-wave (FMCW) radars have recently been proposed for vital-sign monitoring [5]. These systems have range resolution—i.e., they can estimate absolute distances—, leading also to range-bin isolation capabilities [5].

To make an FMCW radar a coherent system is not trivial, since it requires to share the clocks at the generation and acquisition stages [5]. However, if the coherence property for the FMCW radar is achieved, the phase history of targets is preserved during the coherent processing interval (CPI) and Doppler information can thus be derived. This provides the system with two dimensions—i.e., the range and the Doppler—, which can be used to isolate more easily the wanted targets from surrounding clutter.

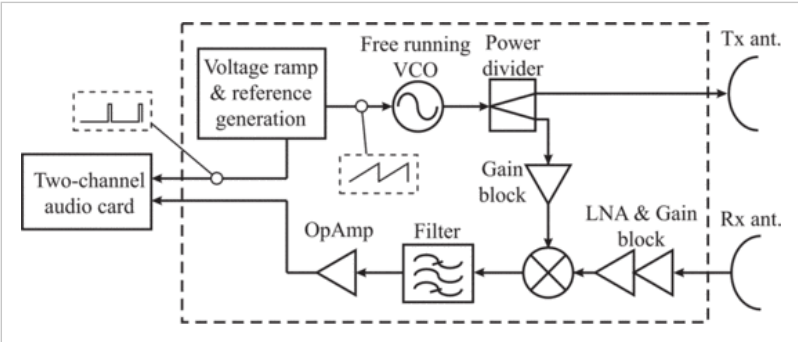


Fig. 1. Simplified block diagram of the portable FMCW radar.

locked to tuning voltage of the voltage controlled oscillator (VCO). This leads to simplicity in terms of the fact that the generation and acquisition clocks can be different—i.e., the analog-to-digital converter (ADC) can work with its internal clock, that is independent of that of the radar signal generator.

Experimental results—consisting of video frames obtained after applying a method to reconstruct inverse synthetic aperture radar (ISAR) images—enable to verify the coherence of the radar and the possibility to track the echoes of a walking person in the 2D range-Doppler domain for indoor healthcare applications.

SECTION II

DESCRIPTION OF THE RADAR PROTOTYPE

A high-level architecture for the 5.8-GHz radar prototype is shown in Fig. 1. The dashed box groups together the RF and baseband circuits in two PCB substrates with a total volume of $60\text{mm} \times 50\text{mm} \times 15\text{mm}$. The transmission (Tx) and reception (Rx) radiation elements are two wideband Vivaldi antennas. The acquisition block is comprised by the audio card in a laPtoP.

The Tx baseband generation block uses simple operational-amplifier-based electronics to obtain two signals with the same period: a voltage sawtooth signal and a pulsed one—i.e., the reference signal—to be acquired by the audio card. The voltage sawtooth signal excites a free-running VCO which outputs the C-band chirps to be subsequently transmitted. The RX part proceeds with the mixing of a replica of the transmitted signal—which is derived from a power divider—with the received echoes. This is the so-called analog deramping technique [5], giving rise to a narrow-band baseband signal, which can be easily acquired by a low-end ADC—note that the sampling frequency of the audio card is only $f_s = 44.1\text{kHz}$ —. Before acquisition, the baseband signal is adequately filtered and amplified, as shown in Fig. 1.

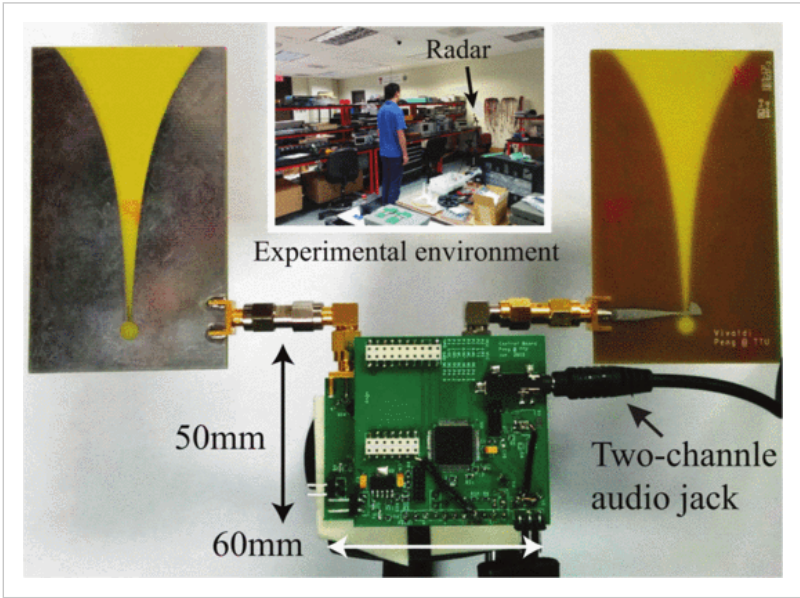


Fig. 2. Photograph of the portable coherent FMCW radar prototype. Inset: Highly-cluttered experimental environment.

| | |
|-------------------------------|----------|
| Center frequency (f_c) | 5.8 GHz |
| Transmitted bandwidth (B) | 300 MHz |
| Transmitted average power | 8 dBm |
| Waveform period (T) | 15.2 ms |
| Sampling frequency (f_s) | 44.1 kHz |

Table I Parameters of the coherent FMCW radar prototype

A photo of the low-cost compact radar prototype is provided in Fig. 2. The simultaneous sampling of the reference and baseband signals enables a correct formatting of the baseband-signal samples to construct the raw-data matrix [5]. This is a simple solution which guarantees the coherence of the system, without the necessity of sharing clocks between the generation and acquisition blocks.

The parameters of the radar are detailed in Table I. The chirp rate can be calculated as $\gamma = B/T = 2 \cdot 10^{10}\text{Hz/s}$. The range resolution is given by $\Delta_R = c/(2B) = 0.5\text{m}$, with c being the speed of light. The maximum non-ambiguous range—note that the baseband signal is a real-valued signal—is provided by $R_{\text{max}} = c \cdot f_s / (4 \cdot B) = 165.4\text{m}$. Finally, as widely known, the Doppler frequency is contained in the interval $[-0.5/T, 0.5/T]$, which gives rise to

a maximum non-ambiguous velocity for moving targets of $v_{\max} = \lambda/(4T) = 0.85\text{m/s}$, where λ is the wavelength for the transmitted center frequency ($\lambda = c/f_c$).

SECTION III

CONSTRUCTION OF THE ISAR VIDEO

As detailed in Section II, the construction of the raw-data matrix is accomplished by detecting the beginning of each ramp with the help of the reference pulsed signal. For each transmitted period T , there are a total of $N = \lfloor T \cdot f_s \rfloor$ fast-time samples. Additionally, the number of slow-time instants is $M = \lfloor CPI/T \rfloor$. Thus, the raw-data matrix $\mathbf{M}_r[m, n]$ has M rows and N columns [5].

Since the range information for a deramping-based FMCW radar is contained in the frequency of the baseband signal, a Fourier transform applied to each row of the raw-data matrix gives rise to the corresponding range-profile matrix—i.e., the range-slow-time map $\mathbf{M}_{rp}[m, q]$, where q is the index to the bins of the fast-time frequency—. The first frame of the ISAR video can be obtained by taking the first M_{chip} range profiles—i.e., $\mathbf{M}_{rp}[m_1, q]$, where $m_1 = \{1, 2, \dots, M_{chip}\}$ with $M_{chip} \ll M$ —and applying to this matrix a column-wise Fast Fourier Transform (FFT).

The application of this Fourier transform gives rise to the first frame of the ISAR image—i.e., a range-Doppler matrix—, since the frequency associated with the slow-time is the Doppler frequency [5]. Obtaining the next frames of the ISAR video simply requires taking M_{chip} consecutive range profiles from the complete complex-valued range-slow-time matrix $\mathbf{M}_{rp}[m, q]$ and applying the corresponding column-wise FFT. In this procedure, some of the M_{chip} consecutive range profiles for the current ISAR frame can be overlapped with some of the previous ISAR image, if desired.

To obtain the range profiles and the range-Doppler ISAR frames, the zero-padding technique can be applied both to the fast- and slow-time [5]. As known, this procedure provides more points in the transformed domains, leading to a better estimation of the point spread function (PSF) of targets. To reduce secondary lobes which could mask weak returns from the desired target, conventional windowing—Hanning weighting—can also be applied.

SECTION IV

EXPERIMENTAL RESULTS

The radar prototype was used to illuminate a walking person which was slowly moving away from the radar and then returning back to it. The indoor scenario was a laboratory with many stationary clutter returns—see inset in Fig. 2. The parameters for the ISAR-video-generation procedure are listed in Table II.

Fig. 3 shows the range-profile matrix $\mathbf{M}_{rp}[m, q]$ for the acquisition. Many vertical strips corresponding to stationary clutter returns can be observed. Also, the echoes from the walking subject are identifiable as tilted returns in this range-slow-time map.

A frame of the ISAR video when the person was walking away from the radar is detailed in Fig. 4(a). As a proof of the coherence feature of the low-cost FMCW radar prototype, the zero-Doppler echoes corresponding to the stationary clutter are clearly observable. Besides, the echo associated with the person can be seen as a blob in a specific range-Doppler position. The fact of having Doppler information together with the ability of detecting absolute ranges provides the system with 2D isolation and tracking capabilities. This could be leveraged for radar-based indoor healthcare applications.

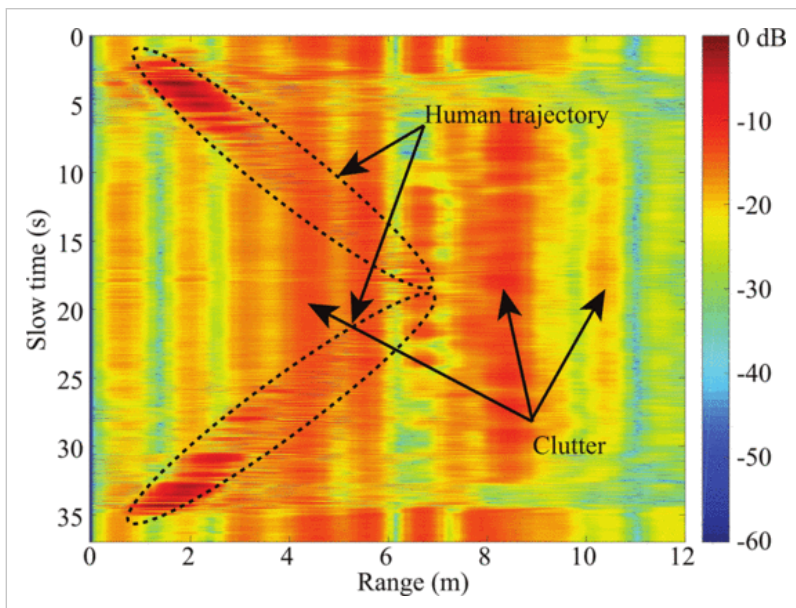


Fig. 3. Range-profile matrix $\mathbf{M}_{rp}[m, q]$ for the experiment.

Loading [MathJax]/extensions/MathZoom.js

| | |
|--|---------|
| Coherent Processing Interval (CPI) | 23.1 s |
| Effective number of fast-time samples (N_{ef}) | 576 |
| Number of slow-time instants (M) | 1528 |
| Reduced number of range profiles (M_{chip}) | 64 |
| Number of row-wise FFT points | 4096 |
| Number of column-wise FFT points | 512 |
| Windowing type | Hanning |

Table II Parameters for ISAR video generation

Fig. 4(b) depicts a frame of the ISAR video when the subject was walking back to the radar. Again, the zero-Doppler returns correspond to the stationary clutter, whereas the moving-target echo has a Doppler frequency with a sign opposite to the result in Fig. 4(a). The echoes observed around the main return in Figs. 4(a) and 4(b) correspond to the micro-Doppler features of the human gait [6].

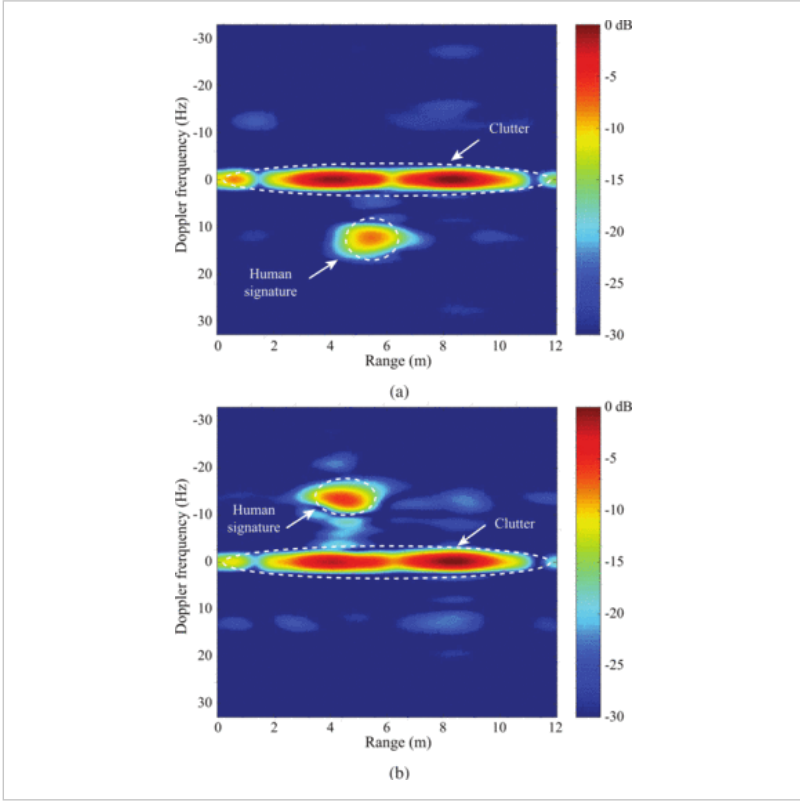


Fig. 4. (a) A frame of the ISAR video when the walking person is moving away from the radar. (b) A frame of the ISAR video when the walking subject is walking back to the radar.

SECTION V CONCLUSION

The use of a coherent FMCW radar prototype for indoor healthcare applications has been reported. A unique feature of this portable low-cost system is the preservation of the phase/Doppler histories of targets by simultaneously acquiring the baseband and reference signals. Experimental results consisting of inverse synthetic aperture radar (ISAR) video frames have also been demonstrated.

Acknowledgment

This work was supported in part by the National Science Foundation (NSF) under grant ECCS-1254838, the Texas Tech University Global Scholar Academy program, the University of Alcalá under Project CCG-2014/EXP-021, and the Spanish Ministry of Economy and Competitiveness under Project TEC2014-54289-R.

FOOTNOTES

No Data Available
Loading [MathJax]/extensions/MathZoom.js

REFERENCES

1.

J. M. Muñoz-Ferreras, Z. Peng, R. Gómez-García, G. Wang, C. Gu and C. Li

"Isolate the clutter: Pure and hybrid linear-frequency-modulated continuous-wave (LFMCW) radars for indoor applications"

IEEE Microw. Mag., vol. 16, no. 4, pp. 40-54,

[Show Context](#)

2.

C. Li, V. M. Lubecke, O. Boric-Lubecke and J. Lin

"A review on recent advances in Doppler radar sensors for noncontact healthcare monitoring"

IEEE Trans. Microw. Theory Techn., vol. 61, no. 5, pp. 2046-2060,

[Quick Abstract](#) | [Show Context](#) | [Full Text: PDF](#)

3.

M. Mercuri, D. Schreurs and P. Leroux

"SFCW microwave radar for in-door fall detection"

Proc. IEEE Topical Conf. Wireless Sensors Sensor Networks (WiSNet), pp. 53-56,

[Quick Abstract](#) | [Show Context](#) | [Full Text: PDF](#)

4.

L. Liang, M. Popescu, M. Rantz and M. Skubic

"Fall detection using Doppler radar and classifier fusion"

Proc. IEEE-EMBS Int. Conf. Biomedical Health Informatics, pp. 180-183,

[Quick Abstract](#) | [Show Context](#) | [Full Text: PDF](#)

5.

G. Wang, J. M. Muñoz-Ferreras, C. Gu, C. Li and R. Gómez-García

"Application of linear-frequency-modulated continuous-wave (LFMCW) radars for tracking of vital signs"

IEEE Trans. Microw. Theory Techn., vol. 62, no. 6, pp. 1387-1399,

[Quick Abstract](#) | [Show Context](#) | [Full Text: PDF](#)

6.


V. C. Chen

The Micro-Doppler Effect in Radar

2011, Artech House


[Show Context](#)

AUTHORS




Zhengyu Peng

No Bio Available




José-María Muñoz-Ferreras

No Bio Available




Yao Tang

No Bio Available



Roberto Gómez-García

No Bio Available



Changzhi Li

No Bio Available

CITED BY

None

KEYWORDS

IEEE Keywords

Doppler effect, Doppler radar, Legged locomotion, Prototypes, Radar tracking, Videos

INSPEC: Controlled Indexing

geriatrics, health care, image reconstruction, indoor navigation, medical signal processing, radar imaging, radar tracking, synthetic aperture radar, video signal processing

INSPEC: Non-Controlled Indexing

FMCW radar prototype, ISAR images, absolute-range detection capabilities, acquisition clocks, elderly people, fall detection, generation clocks, image reconstruction, indoor healthcare scenarios, indoor human tracking, inverse synthetic aperture radar, phase history, portable coherent frequency-modulated continuous-wave radar, radar-based human tracking, range-Doppler frames, videos, walking person

Authors Keywords

Coherent radars, frequency-modulated continuous-wave (FMCW) radars, indoor scenarios, inverse synthetic aperture radar (ISAR)

CORRECTIONS

None

IEEE Account

- » Change Username/Password
- » Update Address

Purchase Details

- » Payment Options
- » Order History
- » View Purchased Documents

Profile Information

- » Communications Preferences
- » Profession and Education
- » Technical Interests

Need Help?

- » **US & Canada:** +1 800 678 4333
- » **Worldwide:** +1 732 981 0060
- » Contact & Support

About IEEE *Xplore* | Contact Us | Help | Terms of Use | Nondiscrimination Policy | Sitemap | Privacy & Opting Out of Cookies

A not-for-profit organization, IEEE is the world's largest technical professional organization dedicated to advancing technology for the benefit of humanity.
© Copyright 2017 IEEE - All rights reserved. Use of this web site signifies your agreement to the terms and conditions.